

**ULYSSES FIELD AND PLASMA OBSERVATIONS OF MAGNETIC HOLES IN
THE SOLAR WIND AND THEIR RELATION TO
MIRROR-MODE STRUCTURES**

Daniel Winterhalter, Marcia Neugebauer, Bruce E. Goldstein, and Edward J. Smith
Jet Propulsion Laboratory, California Institute of Technology, Pasadena, CA 91109

Samuel J. Bame

Los Alamos National Laboratory, Los Alamos, NM 87545

Andre Balogh

Blackett Laboratory, Imperial College, London SW72BZ, UK

Submitted to *J. Geophys. Res.* April 5, 1994

ULYSSES FIELD AND PLASMA OBSERVATIONS OF MAGNETIC HOLES IN THE SOLAR WIND AND THEIR RELATION TO MIRROR-MODE STRUCTURES

Daniel Winterhalter, Marcia Neugebauer, Bruce E. Goldstein, and Edward J. Smith
Jet Propulsion Laboratory, California Institute of Technology, Pasadena, CA 911 09

Samuel J. Bame
Los Alamos National Laboratory, Los Alamos, NM 87545

Andre Balogh
Blackett Laboratory, Imperial College, London SW72BZ, UK

ABSTRACT

The term “magnetic hole” has been used to denote isolated intervals when the magnitude of the interplanetary magnetic field drops to a few tenths, or less, of its ambient value for a time that corresponds to a linear dimension of tens to a few hundreds of proton gyro-radii. Data obtained by the Ulysses magnetometer and solar wind analyzer have been combined to study the properties of such magnetic holes in the solar wind between 1 AU and 5.4 AU and to 23° south latitude. In order to avoid confusion with decreases in field strength at interplanetary discontinuities, the study has focused on linear holes across which the field direction changed by less than 5°. The holes occurred preferentially, but not without exception, in the interaction regions on the leading edges of high-speed solar wind streams. Although the plasma surrounding the holes was generally stable against the mirror instability, there are indications that the holes may have been remnants of mirror mode structures created upstream of the points of observation. Those indications include: (1) For the few holes for which proton or alpha-particle pressure could be measured inside the hole, the ion thermal pressure was always greater than in the plasma adjacent to the holes. (2) The plasma surrounding many of the holes was marginally stable for the mirror mode, while the plasma environment of all the holes was significantly closer to mirror instability than was the average solar wind. (3) The plasma containing trains of closely spaced holes was closer to mirror instability than was the plasma containing isolated holes. (4) The near-hole plasma had much higher ion β (ratio of thermal to magnetic pressure) than did the average solar wind. (5) Near the holes, T_{\perp}/T_{\parallel} tended to be either >1 or larger than in the average wind, (6) The proton and alpha-particle distribution functions measured inside the holes occasionally exhibited the

flattened phase-space-density contours in v_{\perp} - v_{\parallel} space found in some numerical simulations of the mirror instability.

INTRODUCTION

The term “magnetic hole” was introduced by *Turner et al.* [1977] to describe localized depressions in the magnitude of the interplanetary magnetic field (IMF) observed in 1971 by Explorer 43 (also known as IMP 6). The holes were defined as dips in the field magnitude to less than 1 nT detected in plots of data averaged over 15-s intervals (the detailed definition used in the present paper is different; see the analysis section). Their study found 28 magnetic holes in 18 days of data. The holes were distinct entities in otherwise nearly average IMF conditions; i.e., they were not random depressions in a region of noisy or weak fields. The widths of the holes ranged from 2 to 130 s, with a median of 50 s, corresponding to thickness in the solar radial direction of ~ 200 proton gyro radii. Nine of the holes showed large angle changes with evidence for **sub-Alfvénic instreaming** and **field** reconnection, Eight of the 28 holes, however, exhibited little or no directional change; such structures were named **linear** holes. The linear holes were observed in regions of high plasma $\beta = nkT/(B^2/8\pi)$, and all but one of them occurred on or near the leading edges of high-speed streams in the solar wind. Turner et al. suggested that the linear holes, which could not have been caused by reconnection, resulted from the diamagnetic response of the **field** to **local** plasma inhomogeneities, but the cause of the inhomogeneities remained an open question.

In a follow-on study, *Fitzenreiter and Burlaga* [1978] analyzed magnetic holes observed by both the IMP 5 and IMP 6 spacecraft. Combination of the data from the two spacecraft demonstrated consistency with planar current sheets with no significant curvature over a distance of $\sim 2 \times 10^5$ km. For each of the holes analyzed, however, the field rotated by $> 90^\circ$, and thus the conclusions concerning planar structure do not necessarily apply to linear holes. By assuming that the linear holes are also planar structures, *Fitzenreiter and Burlaga* went on to show that the shape and thickness of the currents on the edges of linear holes agree with those deduced by *Burlaga and Lemaire* [1978] from their self-consistent solution of the Vlasov and Maxwell equations in one dimension.

Klein and Burlaga [1980] found that magnetic holes tend to be concentrated near stream interfaces where fast streams overtake the slower ambient wind. That study did not distinguish between linear and rotational holes, however. They suggested that the holes might be due to instabilities associated with the interface or to material trapped between adjacent converging flows near the Sun.

Clues to the origin and nature of magnetic holes in the solar wind can perhaps be obtained from studies of similar features observed in the Earth's magnetosheath. *Kaufmann et al. [1970]* were the first to study dropouts in field magnitude in the magnetosheath. Using Explorer-12 data, they showed that the dips in field strength were anti-correlated with the flux of electrons with energy >200 eV (there were no lower-energy plasma data from that spacecraft), and interpreted the structures as slow-mode magnetoacoustic waves, while admitting the possibility of standing pressure-balance structures. Kaufmann et al. went on to suggest that the mirror instability might be the underlying cause of the features. Using data from IMP 6, *Crooker et al. [1979]* showed that the anisotropy of the plasma depletion layer just outside the magnetopause was usually unstable to the mirror mode. *Tsurutani et al. [1982]* used data from ISEE 1 and 2 to show that the quasi-periodic dips in field strength in the magnetosheath did, in fact, meet the high β and $T_{\perp}/T_{\parallel} > 1$ criteria for the mirror instability. Subsequent observations of variations in the magnitude of the magnetic field credited to the mirror instability have been made in the near-Earth magnetosheath [*Hubert et al., 1989; Hubert et al., 1989; Lacombe et al., 1992; Anderson and Fuselier, 1993*], in the far-downstream terrestrial magnetosheath [*Tsurutani et al., 1984*], in the magnetosheaths of Jupiter and Saturn [*Tsurutani et al., 1982; Balogh et al., 1992*], and in the cometosheath of comet Halley [*Russell et al., 1987*].

Against this background of magnetosheath observations, *Tsurutani et al. [1992]* interpreted a series of magnetic dips (which they did not call "magnetic holes") observed by Ulysses in the plasma behind an interplanetary shock as being caused by the mirror instability. The ion β during that period was high (~ 4), but the plasma anisotropy was not examined.

The mirror instability occurs when both the plasma β and the temperature anisotropy (T_{\perp}/T_{\parallel}) are large (the larger β , the less anisotropy is required). Theoretically, the instability was first treated as a magnetohydrodynamic instability [*Rudakov and Sagdeev, 1961; Thompson, 1964*], but was later described more accurately with a kinetic approach [*Tajiri, 1967; Hasegawa, 1969*] by which it was shown that the mirror instability selectively affects the portion of the particle distribution with large pitch angles. Recently, further elucidating the kinetic approach, *Southwood and Kivelson [1993]* described the physical mechanism of the instability in terms of the behavior of the large pitch angle particles which play the role of "resonant" particles.

Linear Vlasov theory predicts that $T_{\perp}/T_{\parallel} > 1$ also leads to the growth of the proton cyclotron instability. This growing mode has a lower threshold anisotropy at intermediate and low β [*Gary et al., 1976*], implying that the mirror instability should be observed

only above some critical value of β . *Price et al. [1986]* have shown that the presence of alpha particles introduces damping of the proton cyclotron instability while leaving the mirror mode unaffected, thereby reducing the critical β value. *Anderson and Fuselier [1993]* found that in the subsolar magnetosheath the critical value of the parallel proton beta, β_{\parallel} , is about two or three; below that value proton-cyclotron-like fluctuations predominated whereas mirror-like fluctuations were primarily observed above that critical value.

Because linear theory predicts that the relationship between these two instabilities is a sensitive function of the relative helium ion concentration [*Gary et al., 1993*], it would be interesting to study the effect of this concentration on the possible growth of the mirror instability.

In this paper we **pursue** the question of the possible relation of magnetic holes in the solar wind to the mirror instability and compare the data to the results of numerical simulations and theory. The methodology was: (1) to search 26 months of solar-wind data acquired by the magnetometer on Ulysses for magnetic holes, (2) to compile statistics concerning their nature and occurrence rate as a function of distance from the Sun and relative to the solar wind stream structure, (3) to select a subset of linear holes that were reasonably simple and isolated from other field variations, calculate the mirror instability criterion for each event in the subset, and compare the results to the average wind observed by Ulysses, and (4) to examine the ion distribution functions within the holes. The detailed study was limited to linear holes to minimize confusion with dips in field magnitude caused by reconnection or other processes associated with interplanetary discontinuities.

OBSERVATIONS

INSTRUMENTATION

The Ulysses magnetometer experiment utilizes both a tri-axial fluxgate magnetometer and a vector helium magnetometer [*Balogh et al., 1992*]. The experiment usually returns one vector per second, although, when allowed by the spacecraft data rate, can return two vectors per second. The magnetometers have been in nearly continuous operation since shortly after launch.

The plasma data were obtained by the Ulysses solar wind plasma experiment Solar Wind Observations Over the Poles of the Sun (SWOOPS). The design and operation of SWOOPS are described by *Bame et al. [1992]*. In its usual mode of operation, SWOOPS measures the three-dimensional distribution of protons and alphas with resolution of 5% in energy and -5° in both polar and azimuthal angles. The ion data are acquired by mea-

asuring the two-dimensional angular distributions for each of four consecutive energy levels during a single 12-s spin of the spacecraft. A complete, 40-energy-level spectrum is acquired over ten consecutive spins (i.e., over 2 minutes). A 2-minute spectrum is obtained every 4 or 8 rein, depending on whether the spacecraft is being tracked or is storing data for later readout, SWOOPS has been in nearly continuous operation since November 18, 1990, when Ulysses was 1.15 AU from the Sun, but notational motion of the spacecraft between November 18 and December 18, 1990, prevented determination of the three-dimensional distribution functions for that period.

STATISTICAL ANALYSIS

An example of a magnetic hole is given in Figure 1a, showing 1-second-average Ulysses magnetometer data. Figure 1b displays the same event expanded along the time axis by a factor of 16, showing that the hole is indeed resolved with 7 data points. The field magnitude dropped precipitously from about 9.5 nT to less than 3.0 nT in about 7 seconds. In this example there was little or no rotation of the field as it decreased: the solar-ecliptic x and y components (there is no z component in this example) decreased in phase with each other. Also note the three or four small inverted spikes following the hole which look in all respects much like the hole except the decrease was much less.

The appearance of holes in the magnetic field data is varied. Figure 2 shows five unrelated intervals, each of which contains magnetic holes of different structures, all with field rotations less than 5°. As it turns out, the events with no field rotation are those most easily recognized as magnetic holes, often appearing as isolated or small wave train events in a quiet background. The holes depicted in Figure 2 range from what could be described as short wave trains (a and b), to single events reminiscent of solitons. All have a quiet magnetic field background, with the exception of Figure 2c, where the noisy background may disguise a wave train of magnetic holes.

In order to gather statistical information about the magnetic holes, Ulysses magnetic field data (one second averages) covering the period from launch to the end of 1992 were electronically scanned. A hole was defined to be a dip' in the field strength such that $B_{\min}/B_0 \leq 0.5$ where B_{\min} and B_0 are the minimum and average field magnitudes within a sliding window 300 seconds in length. The defining values of B_{\min}/B_0 and the window length were arrived at by trial and error, noting that with values of 0.5 and 300s, respectively, the program found most of the magnetic holes that were visually apparent in plots of time series data. The program also determined the width δt of each hole, in seconds, as well as the field rotation $\delta\theta$ across the hole.

The search program found 4127 magnetic holes during the 26 month period Oct. 1990 to Dec. 1992, including 428 events downstream of the Jovian bow shock. In the solar wind, outside the Jovian environment, there were typically about 100 events per month (Figure 3). This large number probably reflects the simplicity of the selection procedure. We know the selected sample includes many magnetic holes, but there are also probably contributions from heliospheric current sheet crossings [*Winterhalter et al.*, 1993] and from other phenomena that produce field decreases but that are not commonly considered to be magnetic holes. On the other hand, all the events represent significant, short-lived decreases of the field magnitude, so it is conceivable that they all involve the same underlying physical mechanism.

Magnetic holes were found over the full ranges of heliocentric distance and latitude sampled by Ulysses through 1992. Figure 3 shows that the rate of occurrence was highly variable. There is no obvious indication in Figure 3 that the occurrence of holes was related to heliocentric distance. There is a suggestion, however, that the number of holes may have increased with latitude, although this point requires further analysis of higher latitude Ulysses data.

The rotation of the magnetic field vector across a hole ($\delta\theta$) was usually small (Figure 4), with more than 30% of the holes having rotations less than 10° . If we restrict the selection to cases in which the rotation of the magnetic field vector across the hole was small (“linear holes”), say $50 < \delta\theta < 5^\circ$, the average number of events per month was 33, which is greater than the number of linear holes observed near 1 AU over a much shorter interval by *Turner et al.* [1977].

The number of holes decreased with B_{\min}/B_0 , which is a reasonable trend. There were 40 holes with $B_{\min}/B_0 < 0.05$, and approximately 800 holes at the top end of the selection range ($0.45 < B_{\min}/B_0 \leq 0.50$). The average value of B_{\min} decreased with time and heliocentric distance, although at every distance the field sometimes reached very low values. Typically, B_{\min} was about 0.01 nT (Figure 5), but many holes had minimum field strengths that were larger. There were 41 holes with $B_{\min} < 0.005$ nT.

Figure 6 shows the widths of the holes in seconds. The “width” is defined here as the interval that contains the field minimum, and whose start point and end point are one standard deviation below the average field. Typically, the width was between 5 seconds and 25 seconds, with a most probable value lying in the 10-15 seconds bin and a median value of 22s. These numbers compare well with those found by *Turner et al.* [1977], who determined the width of their 28 cases to range from 2 s to 130 s, with a median of 50s. It is important to remember that the geometry of the crossing is not taken into account here, a fact which may contribute to the scatter of the values in Figure 6.

OCCURRENCE OF HOLES RELATIVE TO LARGE-SCALE SOLAR WIND STRUCTURES

To further analyze the properties of the magnetic holes we concentrated on the linear holes across which the magnetic field rotated less than 5° . From the resulting list of 540 events, we then hand-picked 55 cases that occurred in a quiet background and were thus easily identifiable, as those shown in Figures 1 and 2. That list was then cut to the 45 events for which a good plasma spectrum (with no spacecraft nutation) was obtained within 15 minutes of the observation of the hole.

The 45 holes selected for further study were situated in a variety of solar wind settings. Beginning in early May, 1991, when Ulysses was still near the ecliptic at a solar distance of 2.85 AU, through the middle of 1993 (35° south latitude; 4.5 AU), both the magnetometer and SWOOPS data showed the solar wind usually to be divided into distinctive interaction regions (IRs) separated by relatively quiet non-interaction regions (NONIRs) [Smith *et al.*, 1993; Neugebauer *et al.*, 1994]. Of the 32 magnetic holes in our sample observed during that period, 27 were in IRs, 3 were in NONIRs, while 2 were in a region of ambiguous type. Two of the 13 holes observed between Dec. 18, 1990 and May 1, 1991 (i.e., after the cessation of spacecraft nutation but before the regular appearance of well defined IRs and NONIRs) were also in shocked plasma. One of those holes occurred in a region of plasma with $T_\perp > T_\parallel$ extending ~ 4 hours downstream of a strong reverse shock. But other associations can also be found. At least 12 holes were in plasma that could be identified as originating in coronal mass ejections, Seven holes were located in the high-density plasma sheet in which the heliospheric current sheet was usually embedded.

CONSISTENCY WITH MIRROR MODE STRUCTURES

As mentioned in the introduction, features resembling magnetic holes in planetary magnetosheaths have been associated with the mirror instability. One of the purposes of the present study is to determine whether or not the holes detected by Ulysses in the solar wind might have the same origin.

If the magnetic holes are mirror-mode structures, the dip in magnetic pressure must be compensated by an increase in the perpendicular plasma pressure. Because most of the magnetic holes passed by the spacecraft in less than a minute while ion spectra were obtained for 2 minutes out of every 4 or 8 minutes, it was usually not possible to measure the ion density and temperature within a hole. There were a few lucky exceptions, however, when the phasing of the energy sweeps happened to allow the mapping of the peak of either the proton or the alpha-particle distribution (seldom both) within a magnetic hole. There were 8 proton and 5 alpha particle spectra from which in-hole ion densities

and temperatures could be calculated. When those values were compared to the densities and temperatures calculated from adjacent spectra that did not overlap magnetic holes, the results shown in Table 1 were obtained. The first column gives the year, day number, and U'T' of the plasma measurement in the hole. The next two columns give the apparent thickness of the hole ($v\delta t$) in units of either the proton or the alpha gyroradius (R_{Lp} or $R_{L\alpha}$) calculated from the field strength and ion temperature measured inside the hole. The general shape of the time-series plot of magnetic field strength is also noted in those columns, with "simple" indicating a simple v- or u-shaped depression and "double" indicating the appearance of two overlapping holes with more of a w-shape. The last three columns give the ratio of density n , temperature T , and the product nT inside the hole to the corresponding values for a nearby spectrum outside the hole (denoted by subscript o). The data suggest that both the density and temperature usually increased inside a hole, while the thermal pressure was consistently higher inside than outside. It is not possible, however, to carry out a detailed calculation of pressure balance because we do not have simultaneous observations of protons, alphas, and electrons inside the hole.

The stability criterion for mirror mode waves can be stated as a ratio

$$R = \frac{\beta_{\perp}/\beta_{\parallel}}{1 + 1/\beta_{\perp}}$$

where instability corresponds to $R > 1$. Figure 7a shows the distribution of R computed from hourly averages of Ulysses field and plasma data between Dec. 18, 1990 (when the spacecraft nutation stopped) and the end of 1992?. Figure 7b shows the values of R computed from the plasma spectra in the undisturbed plasma adjacent to each of the magnetic holes in our smaller data set. The values of β , T_{\parallel} , and T_{\perp} used to calculate R correspond to total ion values, including protons and alphas, but not electrons. From Figure 7a it is seen that the solar wind is almost always very stable against the mirror instability, with a median value of $R = 0.32$. R exceeded 1.0 for only 4% of the hours in the interval sampled. For the near-hole observations, however, R was usually between 0.5 and 1.0 (Figure 7b), with what amounts to a cut-off near $R=1$. These features are consistent with a state of marginal stability: On the other hand, there are a number of cases which are closer to $R=0.5$ than they are to $R=1$, and it is difficult to argue that the plasma conditions are only marginally stable for those cases. Yet Figure 8 shows that it is primarily single isolated holes (like in Figure 2d and e) that appear to have evolved away from the $R=1$ line, as opposed to multiple holes (like in Figure 2a to c) which cluster more closely around $R=1$. Our interpretation is that Ulysses observed structures generated by mirror mode instabilities which remained after the distribution relaxed to a marginally stable

state. The single holes may be older remnants of wave trains whose other members have decayed away, and whose distribution is much more isotropized.

Further information comparing the state of the solar-wind plasma near magnetic holes to that found during other times is summarized in Table 2. The first row summarizes the data shown in Figure 7. The next two rows contain data on the constituent parts of the instability criterion. T_{\parallel} is almost always greater than T_{\perp} in the solar wind, but on average the plasma adjacent to magnetic holes is as likely to have $T_{\perp}/T_{\parallel} > 1$ as < 1 . We note that *Anderson and Fuselier [1993]* found that mirror instabilities in the sunward magnetosheath were limited to the higher β situations whereas the ion cyclotron instability dominated in lower β plasma. Finally, Table 2 shows that the alpha-particle abundance was slightly lower than average in the near-hole plasma with values of n_{α}/n_p from 0.021 to 0.123.

PARTICLE DISTRIBUTIONS

Figures 9 and 10 display the distribution functions constructed from the few spacecraft spins when the SWOOPS energy-sweep sequence allowed the mapping of the peaks of either the proton or alpha-particle distributions. The distributions correspond to the entries in Table 1, with protons plotted in Figure 9 and alphas in Figure 10. The data were transformed and binned into a two-dimensional coordinate system aligned with the magnetic field and moving with the proton flow speed. Bins containing one or more measurements are marked by a + and contours in regions of phase space with only a few + symbols are not very reliable. There are two contour intervals per decade; i.e., each contour represents a phase space density a factor of 3.16 above or below its neighboring contour.

The contours in Figures 9 and 10 can be compared to the results of numerical simulations by *McKean et al. [1993]* in their Figures 2b and 6g. Both of their simulated distribution functions, one for a slow-growth rate situation and the other for a large-amplitude, rapid-growth case, show rather box-shaped or flattened inner contours in the region of minimum field strength. Some of our distributions (Figures 9g, 9h, 10a, and 10b) exhibit such flattening, but others don't. Our contours do not resemble the distributions proposed by *Southwood and Kivelson [1993]*, but the 5° angular resolution of the SWOOPS instrument (which is coarser than the binning intervals in Figures 9 and 10) would probably smooth out the rather narrow features sketched by Southwood and Kivelson, even if finite gyro-radius effects did not do so, as was suggested by *McKean et al. [1993]*.

From their simulations, *McKean et al. [1993]* also produced contours for the distribution functions on the edges of the holes where the field magnitude was changing rapidly. Examination of the SWOOPS data that overlapped hole edges revealed no evidence of more ions (either protons or alphas) moving into the low field region than moving away from it, as found in the simulations. A possible exception to this statement is shown in Figure 9h, but these observations were obtained almost at the center of the hole.

DISCUSSION AND CONCLUSIONS

The question that naturally arises is what is the origin of the magnetic holes in the solar wind. Some decreases in the magnitude of the interplanetary magnetic field maybe caused by reconnection at tangential discontinuities [*Burlaga, 1968*], while others are associated with quasi-perpendicularly propagating rotational discontinuities with ion-sense rotation [*Neugebauer, 1989*]. The subset of the Ulysses holes selected for detailed analysis 'was, however, limited to linear holes with angular rotation of the field $< 5^\circ$ ', thus eliminating any contribution by or confusion with magnetic reconnection or directional discontinuities.

In principle, a magnetic depression and out-of-phase changes in the field strength and density could be caused by a slow mode wave. We find, however, that the solar wind speed varies little across the holes (< 1 km/s). Thus, there is no evidence for the wave electric field, $\delta E \propto |\delta v \times B|$, necessary for a propagating slow mode wave.

It has been suggested to us that the magnetic holes might have been caused by high-speed impacts of dust with the spacecraft. We believe this interpretation is unlikely. The recurring streams of dust particles [*Grün and al., 1993*] measured by the Ulysses dust experiment appear to be uncorrelated with the magnetic holes in our data set. Furthermore, the distortion of the magnetic field caused by dust impact differs from that of magnetic holes. The magnetic pulses attributed to dust-grain impact on the Giotto spacecraft [*Neubauer et al., 1990*] had time durations of less than a second, compared to tens of seconds for the magnetic holes studied here. Also, the dust-caused dips in field strength observed by Giotto were followed by periods of stronger field, which were not typical of the Ulysses holes,

We believe the linear magnetic holes observed by Ulysses are probably remnants of structures caused by the occasional mirror instability of the solar wind. The reasons for this belief, discussed in more detail in subsequent paragraphs, are: (1) The dip in field strength is accompanied by a simultaneous increase in plasma density and pressure. (2) The holes are found in high β plasma that is significantly less stable to the mirror mode than most of the solar wind, (3) The plasma with trains of closely spaced magnetic holes

is often marginally mirror-mode stable. (4) There is sometimes a similarity of the squared-off velocity-space contours observed within the holes to distribution functions derived from numerical simulations of mirror-mode waves,

The alpha-particles in the solar wind are expected to suppress the growth rate of the ion cyclotron instability which would otherwise be more effective than the mirror instability in reducing the ion anisotropy [Price *et al.*, 1986; Gary *et al.*, 1993]. For the five cases in which alpha-particle data were available inside the holes, the alpha-particle gyro-radius was roughly a quarter of the hole dimension and the velocity distributions of the alphas were similar to those of the protons. Thus the alphas probably participate in the mirror-mode process.

If our interpretation concerning the mirror instability is correct, it leads to the conclusion that the holes are probably created in interplanetary space rather than being a relic solar signal. There is no evidence in Figure 3 that magnetic holes decay or disappear with increasing distance from the Sun. The high, but not perfect, correlation of holes with the interaction regions between forward and reverse shocks supports the hypothesis of interplanetary creation because the shocks associated with corotating high-speed streams do not usually develop until the streams are beyond 1 AU.

Interestingly, a number of the holes found in the solar wind appear to have a single large drop in the field without subsequent oscillations (cf. Figure 2). Other cases had two or three or four oscillations, which were progressively reduced in amplitude. We contrast this to observations of the mirror instability in planetary magnetospheres [Brown *et al.*, 1968], and particularly in the jovian magnetosheath [Balogh *et al.*, 1992], where many field oscillations followed the initial field reduction. In the jovian magnetosheath, the large amplitude waves persisted for days. In the magnetospheric example discussed by Hasegawa [1969], the maximum anisotropy occurred at the minimum magnetic field. It was during the subsequent field oscillations that the plasma anisotropy was reduced. Such features were not seen in the solar wind magnetic holes, perhaps because the initial plasma anisotropy which triggered the instability in the solar wind was not as large as can be found in the magnetosphere or magnetosheath. Another difference between our results in the solar wind and those obtained by other experiments in the magnetosheath is the degree of instability of the plasma. We found the solar wind near magnetic holes to be generally mirror-mode stable, although sometimes only marginally so, wherein Anderson and Fuselier [1993], for example, found the magnetosheath plasma to be unstable. The difference could be the proximity of the holes observed in the magnetosheath to the region (i.e., the bow shock) where the anisotropy was produced. This argument is supported by Figure 8, which shows that in contrast to the single holes, wave trains, short

as they are in the solar wind, cluster closely below the instability threshold. The plasma was, therefore, not yet isotropized (by mechanisms yet to be specified) to the degree shown in plasma with single holes. This process may resemble a sequence in time analogous to Figure 2 (if this figure represented the evolution of a single event, which is dots not), where a small wave train evolves (a) and coalesces into a single hole (e).

Our search has found a large number of magnetic holes in the solar wind. The restriction placed on the identity of the holes, namely that $B_{\min}/B_0 < 0.5$, was arbitrary. We have seen magnetic field signatures in the data which in all respects looked like magnetic holes, except that the dip in the field magnitude was not deep enough to qualify them as such. Because those events were probably formed by the same mechanism, the depth to which the field magnitude drops is of secondary consequence. The term “hole” is perhaps a misnomer because it emphasizes the amount of reduction in the magnetic field. What is important is the underlying mechanism which produces the events whose magnitude depends on the amount of free energy available. Thus we expect a broad range of field decreases and we have likely underestimated the number of magnetic “holes”.

Our analysis suggests that the underlying mechanism is the mirror instability. This instability requires a high plasma β and a temperature anisotropy such that $T_{\perp} > T_{\parallel}$. Such conditions have been observed in many regions of space: behind planetary and interplanetary shocks, in coronal mass ejections, in the heliospheric plasma sheet, in magnetospheres, anywhere near a boundary that influences particle trajectories, etc.; mirror mode structures would be expected to form in such regions. Figure 3 confirms that the number of holes per day is more or less constant in the solar wind, regardless of the appearance and disappearance of particular large scale solar wind structures: there is often something going on in the solar wind that produces high β and $T_{\perp} > T_{\parallel}$. The apparent ubiquity of the mirror instability suggests that it is an important, if not fundamental, mechanism by which space plasmas in all corners of the heliosphere use up free energy.

Many questions remain unanswered. The unknown three-dimensional structure of magnetic holes can perhaps be addressed by studying holes observed by several closely spaced spacecraft such as ISEE 1, 2, and 3. The finding of large-scale planarity by *Fitzenreiter and Burlaga [1978]* was limited to field decreases associated with large field rotations and may well be inapplicable to linear magnetic holes or to any other holes resulting from the mirror instability. Another question is the lifetime of holes in a plasma that is no longer mirror-mode unstable; how long do the structures survive? We do not know how to address such a question observationally, but simulations might be revealing. Another challenge for theoreticians and modelers is to explain the increase of ion temperature within the holes; i.e., how are the ions heated?

ACKNOWLEDGMENTS

We wish to thank S. Peter Gary, Neil Murphy, and Konrad Sauer for their comments and discussions. This research was supported by the Jet Propulsion Laboratory, California Institute of Technology, under contract with the National Aeronautics and Space Administration. Work at Los Alamos was performed under the auspices of the U.S. Department of Energy.

REFERENCES

- Anderson, B. J., and S. A. Fuselier, Magnetic pulsations from 0.1 to 4.0 Hz and associated plasma properties in the Earth's subsolar magnetosheath and plasma depletion layer, *J. Geophys. Res.*, 98, 1461, 1993.
- Balogh, A., T. J. Beek, R. J. Forsyth, P. C. Hedgecock, R. J. Marquedant, E. J. Smith, D. J. Southwood, and B. T. Tsurutani, The magnetic field investigation on the Ulysses mission: Instrumentation and preliminary scientific results, *Astron. Astrophys. Suppl.*, 92, 221, 1992.
- Balogh, A., M. K. Dougherty, R. J. Forsyth, D. J. Southwood, E. J. Smith, B. T. Tsurutani, N. Murphy, and M. E. Burton, Magnetic field observations during the Ulysses flyby of Jupiter, *Science*, 257, 1515, 1992.
- Bame, S. J., D. J. McComas, B. L. Barraclough, J. L. Phillips, K. J. Sofaly, J. C. Chavez, B. E. Goldstein, and R. K. Sakurai, The Ulysses solar wind plasma experiment, *Astron. and Astrophys. Suppl.*, 92, 237, 1992.
- Brown, W. L., L. J. Cahill, L. R. Davis, C. E. McIlwain, and C. S. Roberts, Acceleration of trapped particles during a magnetic storm on April 18, 1965, *J. Geophys. Res.*, 73, 153, 1968.
- Burlaga, L. F., Micro-scale structures in the interplanetary medium, *Solar Phys.*, 4, 67, 1968.
- Burlaga, L. F., and J. F. Lemaire, Interplanetary magnetic holes: Theory, *J. Geophys. Res.*, 83, 5157, 1978.
- Crooker, N. U., T. E. Eastman, and G. S. Stiles, Observations of plasma depletion in the magnetosheath at the dayside magnetopause, *J. Geophys. Res.*, 84, 869, 1979.
- Fitzenreiter, R. J., and L. F. Burlaga, Structure of current sheets in magnetic holes at 1 AU, *J. Geophys. Res.*, 83, 5579, 1978.
- Gary, S. P., S. A. Fuselier, and B. J. Anderson, Ion anisotropy instabilities in the magnetosheath, *J. Geophys. Res.*, 98, 1481, 1993.

- Gary, S. P., M. D. Montgomery, W. C. Feldman, and D. W. Forslund, Proton temperature anisotropy instabilities in the solar wind, *J. Geophys. Res.*, *81*, 1241, 1976.
- Grün, E., and e. al., Discovery of jovian dust streams and interstellar grains by the Ulysses spacecraft, *Nature*, *362*, 428, 1993.
- Hasegawa, A., Drift mirror instability in the magnetosphere, *Phys. Fluids*, *12*, 2642, 1969.
- Hubert, D., C. C. Harvey, and C. T. Russell, Observations of magnetohydrodynamic modes in the Earth's magnetosheath at 06001.1', *J. Geophys. Res.*, *94*, 17305, 1989.
- Hubert, D., C. Perche, C. C. Harvey, C. Lacombe, and C. T. Russell, Observation of mirror waves downstream of a quasi-perpendicular shock, *Geophys. Res. Lett.*, *16*, 159, 1989.
- Kaufmann, R. L., J.-T. Horng, and A. Wolfe, Large-amplitude hydromagnetic waves in the inner magnetosheath, *J. Geophys. Res.*, *75*, 4666, 1970.
- Klein, L., and L. F. Burlaga, Interplanetary sector boundaries 1971-1973, *J. Geophys. Res.*, *85*, 2269, 1980.
- Lacombe, C., F. G. E. Pantellini, D. Hubert, C. C. Harvey, A. Mangeney, G. Belmont, and C. T. Russell, Mirror and Alfvénic waves observed by ISEE 1-2 during crossings of the Earth's bow shock, *Ann. Geophys.*, *10*, 772, 1992.
- McKean, M. E., S. P. Gary, and D. Winske, Kinetic physics of the mirror instability, *J. Geophys. Res.*, *98*, 21313, 1993.
- Neubauer, F. M., K.-H. Glassmeier, A. J. Coates, R. Goldstein, M. H. Acuna, and G. Musmann, Hypervelocity dust particle impacts observed by the Giotto magnetometer and plasma experiments, *Geophys. Res. Lett.*, *17*, 1809, 1990.
- Neugebauer, M., The structure of rotational discontinuities, *Geophys. Res. Lett.*, *16*, 1261, 1989.
- Neugebauer, M., B. E. Goldstein, S. J. Bame, and W. C. Feldman, Ulysses near-ecliptic observations of differential flow between protons and alphas in the solar wind, *J. Geophys. Res.*, *99*, 2505, 1994.
- Price, C. P., D. W. Swift, and L.-C. Lee, Numerical simulation of nonoscillatory mirror waves at the Earth's magnetosheath, *J. Geophys. Res.*, *91*, 101, 1986.
- Rudakov, L. I., and R. Z. Sagdeev, On the instability of a nonuniform rarefied plasma in a strong magnetic field, *Dokl. Akad. Nauk SSSR (Engl. Transl.)*, *6*, 415, 1961.
- Russell, C. T., W. Riedler, K. Schwingenschuh, and Y. Yeroshenko, Mirror instability in the magnetosphere of comet Halley, *Geophys. Res. Lett.*, *14*, 644, 1987.

- Smith, E. J., M. Neugebauer, A. Balogh, S. J. Bame, G. Erdös, R. J. Forsyth, B. E. Goldstein, J. L. Phillips, and B. T. Tsurutani, Disappearance of the heliospheric sector structure at Ulysses, *Geophys. Res. Lett.*, 20, 2327, 1993.
- Southwood, D. J., and M. G. Kivelson, Mirror instability: 1. Physical mechanism of linear instability, *J. Geophys. Res.*, 98, 9181, 1993.
- Tajiri, M., Propagation of hydromagnetic waves in collisionless plasma, II, Kinetic approach, *J. Phys. Soc. Jpn*, 22, 1482, 1967.
- Thompson, W. B., *An Introduction to Plasma Physics*, Pergamon, New York, 1964.
- Tsurutani, B. T., I. G. Richardson, R. P. Lepping, R. D. Zwickl, D. E. Jones, E. J. Smith, and S. J. Bame, Drift mirror mode waves in the distant ($X \approx 200 R_{\odot}$) magnetosheath, *Geophys. Res. Lett.*, 11, 1102, 1984.
- Tsurutani, B. T., E. J. Smith, R. R. Anderson, K. W. Ogilvie, J. D. Scudder, D. N. Baker, and S. J. Bame, Lion roars and nonoscillatory drift mirror waves in the magnetosheath, *J. Geophys. Res.*, 87, 6060, 1982.
- Tsurutani, B. T., E. J. Smith, D. J. Southwood, and A. Balogh, Nonlinear magnetosonic waves and mirror mode structures in the March 1991 Ulysses interplanetary event, *Geophys. Res. Lett.*, 19, 1267, 1992.
- Turner, J. M., L. F. Burlaga, N. F. Ness, and J. F. Lemaire, Magnetic holes in the solar wind, *J. Geophys. Res.*, 82, 1921, 1977.
- Winterhalter, D., E. J. Smith, M. E. Burton, N. Murphy, and D. J. McComas, The heliospheric plasma sheet, *J. Geophys. Res.*, (in press), 1993.

Table 1. Plasma properties of magnetic holes

Yr/Day/UT	$\nu\delta t/KL_p$	$\nu\delta t/KL\alpha$	n/n_0	T/T_0	$nT/(nT)_0$
2010/11/22		27 - complete	1.04	1.01	1.05
2012/11/14	01 - complete		1.01	1.10	1.11
2012/11/14		10 - complete	1.06	1.02	1.11
2012/11/14	17 - complete		1.12	1.02	1.10
2012/11/14	20 - complete		1.00	1.04	1.10
2012/11/14		20 - complete	1.20	1.10	1.30
2012/11/15	20 - Flare	20 - complete	0.77	1.10	1.07
2012/11/17	20 - complete		1.27	1.20	1.51
2012/11/18		24 - complete	2.01	0.84	1.73
2012/11/18	0.5 - complete		1.42	1.04	1.51
2012/11/18		0.1 - complete	2.22	1.00	2.22
2012/11/18	10 - complete		1.42	0.74	1.21
2012/11/18	11 - complete		1.17	1.03	1.18

Table 2. Mean and median values of plasma parameters for the solar wind containing magnetic holes compared to the same parameters for all the solar wind data observed by Ulysses between Dec 18, 1990 and Dec 31, 1992.

Parameter	Magnetic Hole Periods Mean / Median	All Data Mean / Median
$R = \frac{\beta_{\perp}/\beta_{\parallel}}{1 + 1/\beta_{\perp}}$	0.76 / 0.74	0.39 / 0.32
$\frac{T_{\perp}}{T_{\parallel}}$	0.92/0.94	0.90 / 0.82
β	2.90 / 1.74	0.68 / 0.40
n_{α}/n_p	0.054 / 0.045	0.049 / 0.042

FIGURE CAPTIONS

Figure 1. a) Example of a magnetic hole on November 29, 1990. Shown are the magnetic field components in heliographic coordinates, and the field magnitude. b) The same as in a), but with the time scale expanded by a factor of sixteen and centered on the major hole at 02:08:55 UT,

Figure 2. Field magnitude variations in five selected magnetic holes. The events have in common that $B_{\min}/B_0 \leq 0.5$, and $\delta\theta < 5^\circ$ ("linear holes").

Figure 3. The number of magnetic holes found per month in the solar wind and at Jupiter. The total number is 4127, The solar wind events are further subdivided by their magnetic field rotation, The top scales show the monthly averages of Ulysses' heliocentric range and latitude.

Figure 4. Distribution of $\delta\theta$, the angle by which the magnetic field rotated across the magnetic holes in the solar wind. The most probable rotation was in between 3° and 6° . More than 30% of the holes had rotations less than 10° .

Figure 5. Distribution of B_{\min} , the minimum magnetic field strength of each hole, for 3427 solar wind cases. The 272 cases for which $B_{\min} > 1 \text{ nT}$ are not shown. The typical B_{\min} is about 0.01 nT, with 41 holes having $B_{\min} \leq 0.005 \text{ nT}$.

Figure 6. Distribution of the "width", in seconds, across the holes. The width is defined as the interval which contains the field minimum, and whose start point and end point are one standard deviation below the average field. The most probable value was in the 10-15 seconds bin, and the median value was 22s.

Figure 7. Distribution of the stability criterion for mirror mode waves $R = (\beta_{\perp}/\beta_{\parallel})/(1 + 1/\beta_{\perp})$, which is > 1 for instability to occur, for (a) hourly averages of all the solar wind data acquired between Dec. 18, 1990 and Dec. 31, 1992, and (b) in the plasma adjacent to the subset of magnetic holes selected for detailed study.

Figure 8. The total ion temperature an isotropy versus total ion β for the events in Figure 7. Plotted are isolated holes, events that show only one decrease in the magnetic field (open circles), and events that have two or more closely spaced decreases, i.e., multiple holes or wavetrains (solid circles). Also shown is the instability threshold $R=1$ (solid line). Note that the wavetrains tend to cluster near $R=1$.

Figure 9. Contours of proton phase-space density observed inside magnetic holes as a function of v_{\perp} and v_{\parallel} in a coordinate system moving with the solar wind speed and aligned with the interplanetary magnetic field. There are two contours per decade. The + signs mark v_{\perp} - v_{\parallel} bins in which there were measurements.

Figure 10. Same as Figure 9 for alpha-particle distributions.

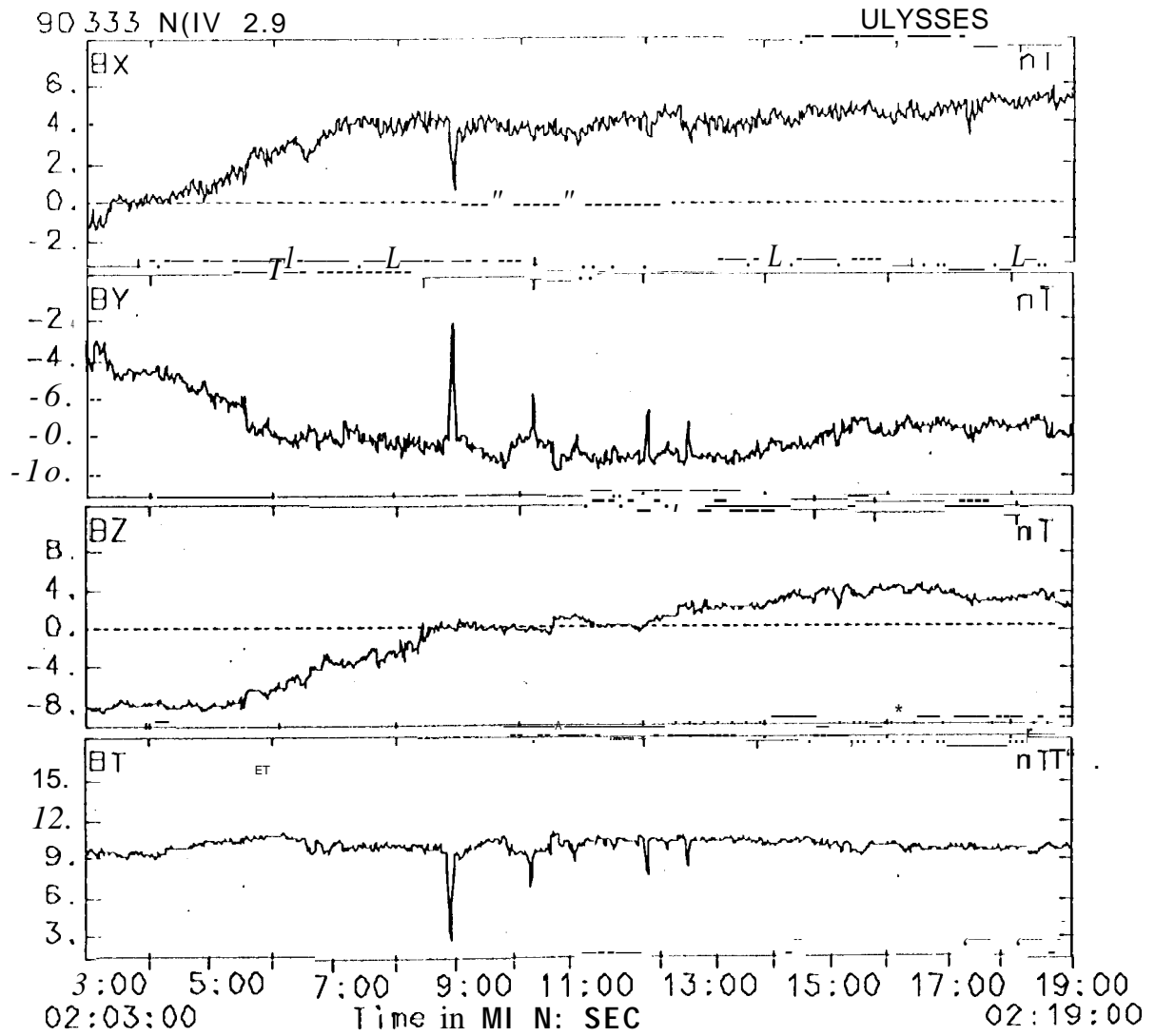


Figure 1a

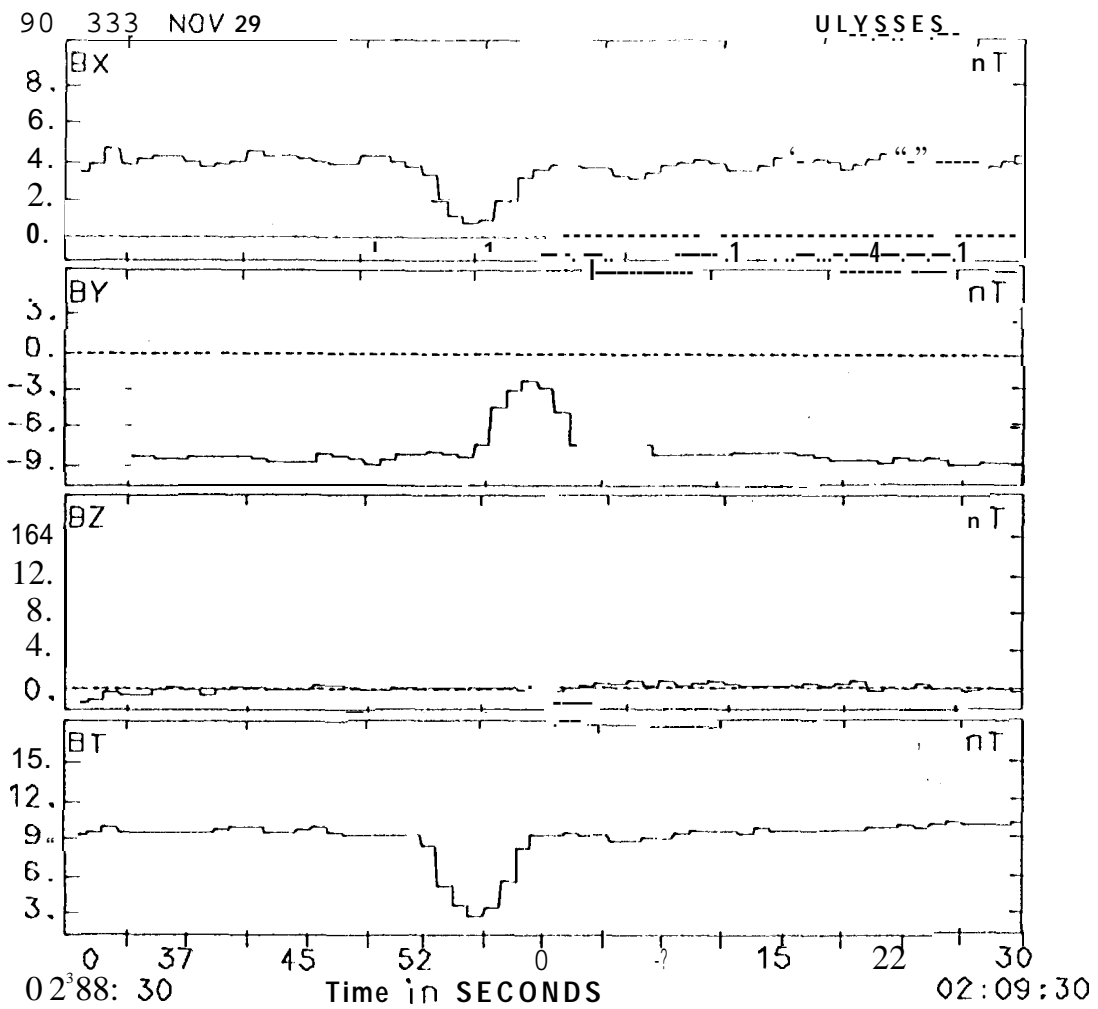


Figure 1 b

Magnetic Field Magnitude [nT]

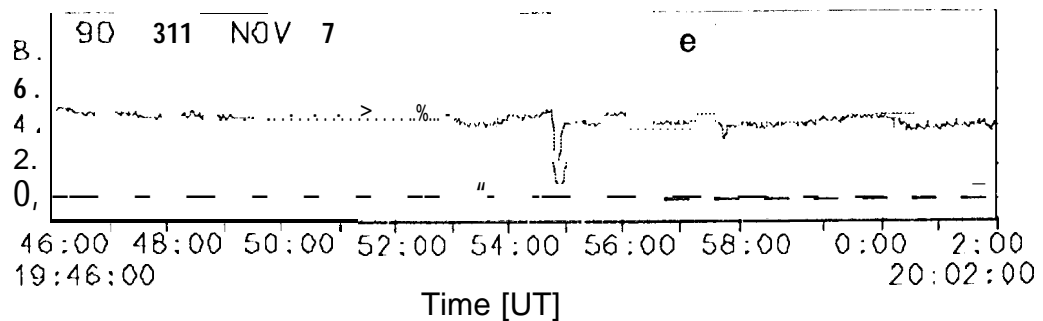
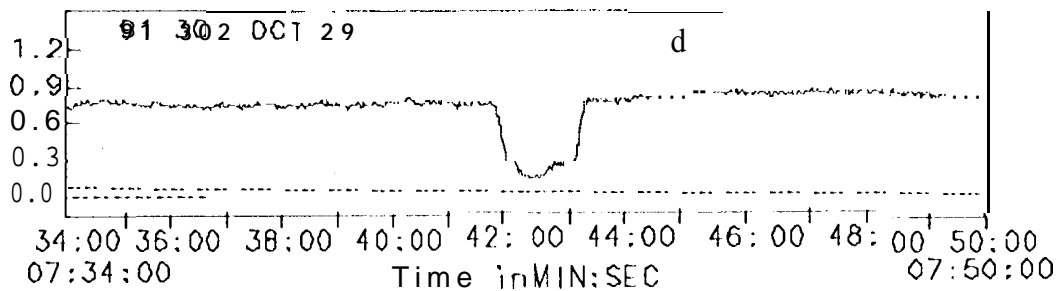
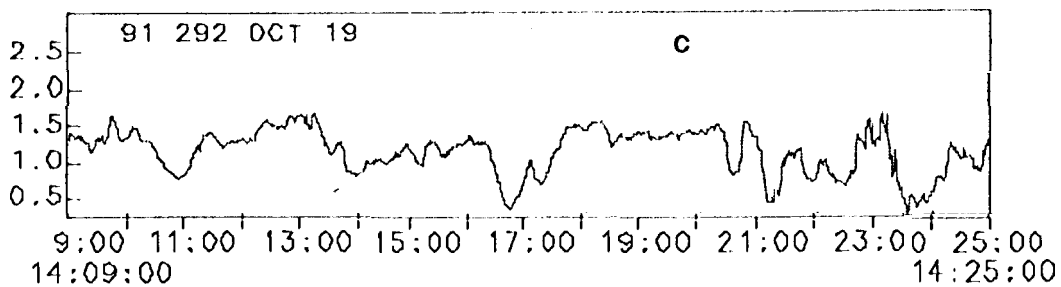
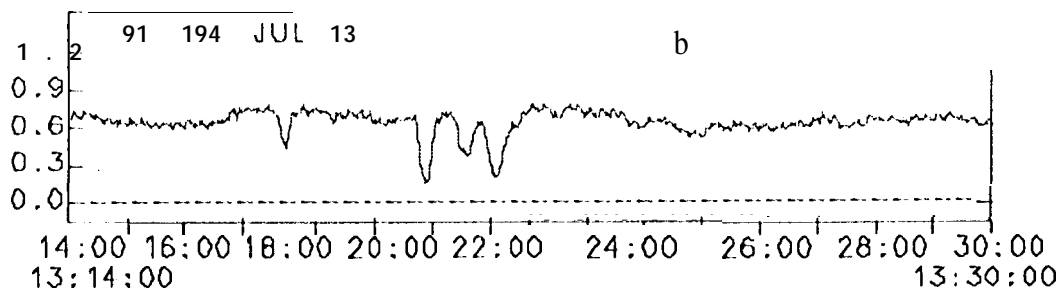
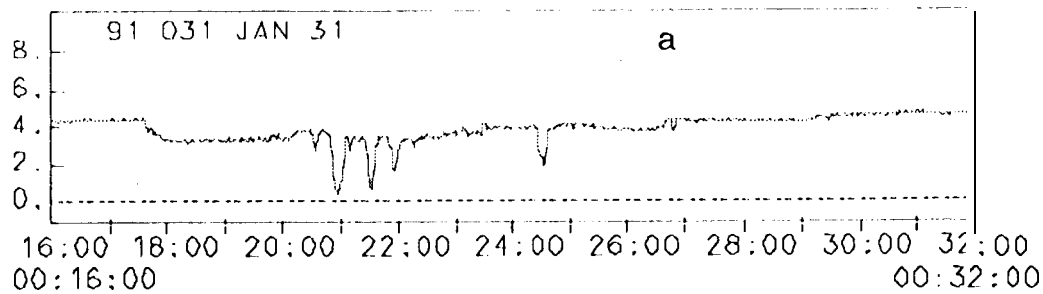


Figure 2

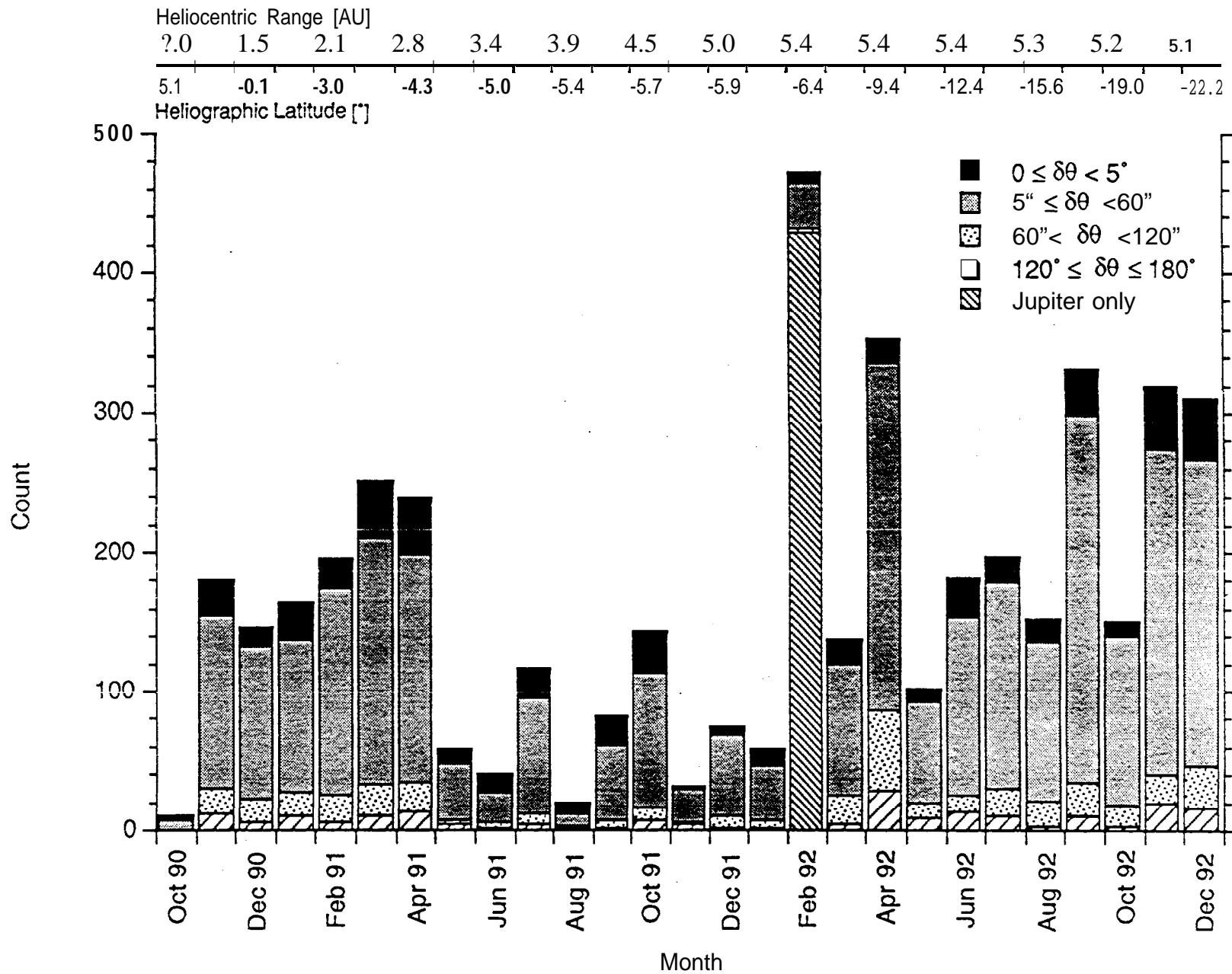


Figure 3

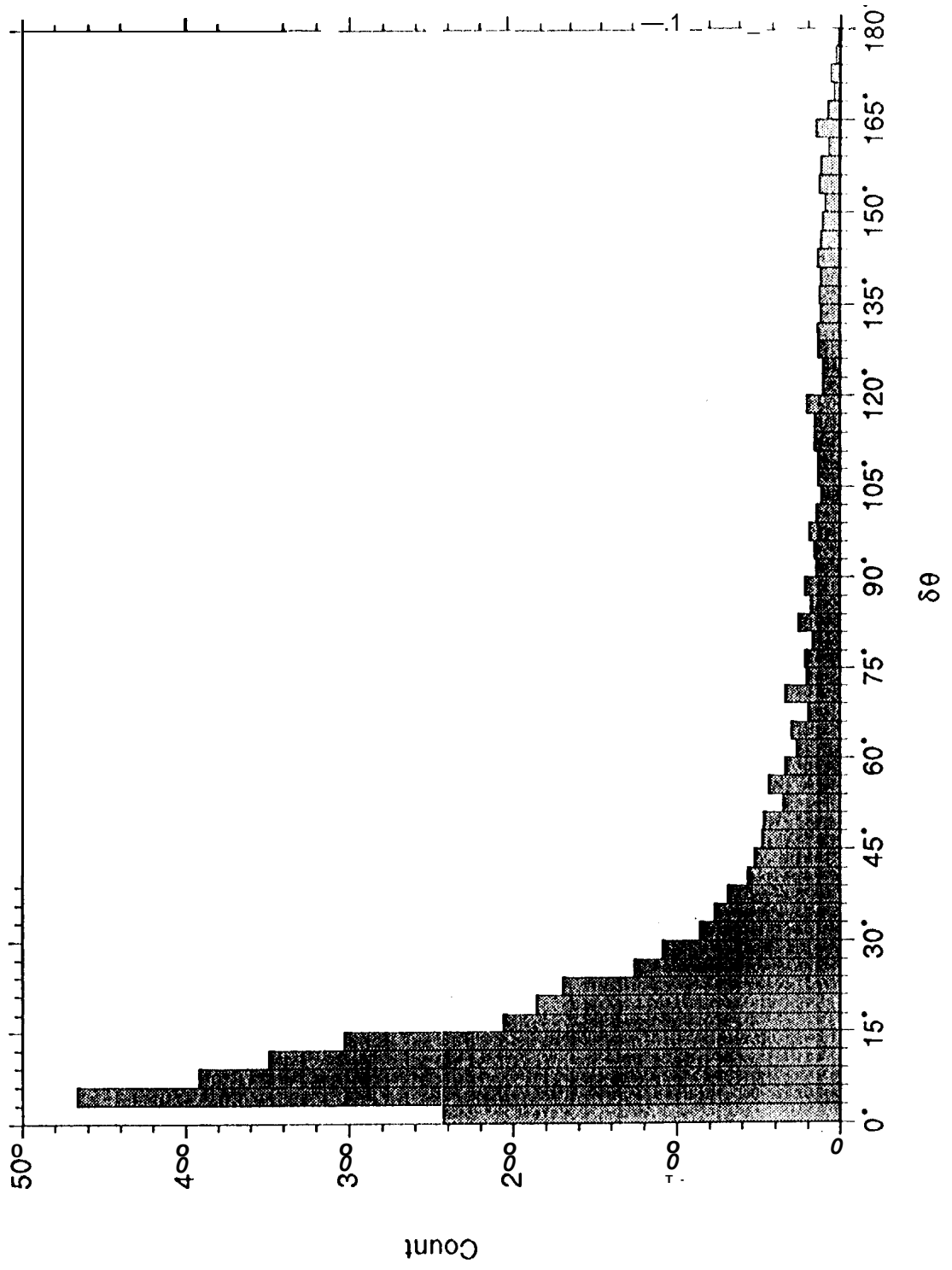


Figure 4

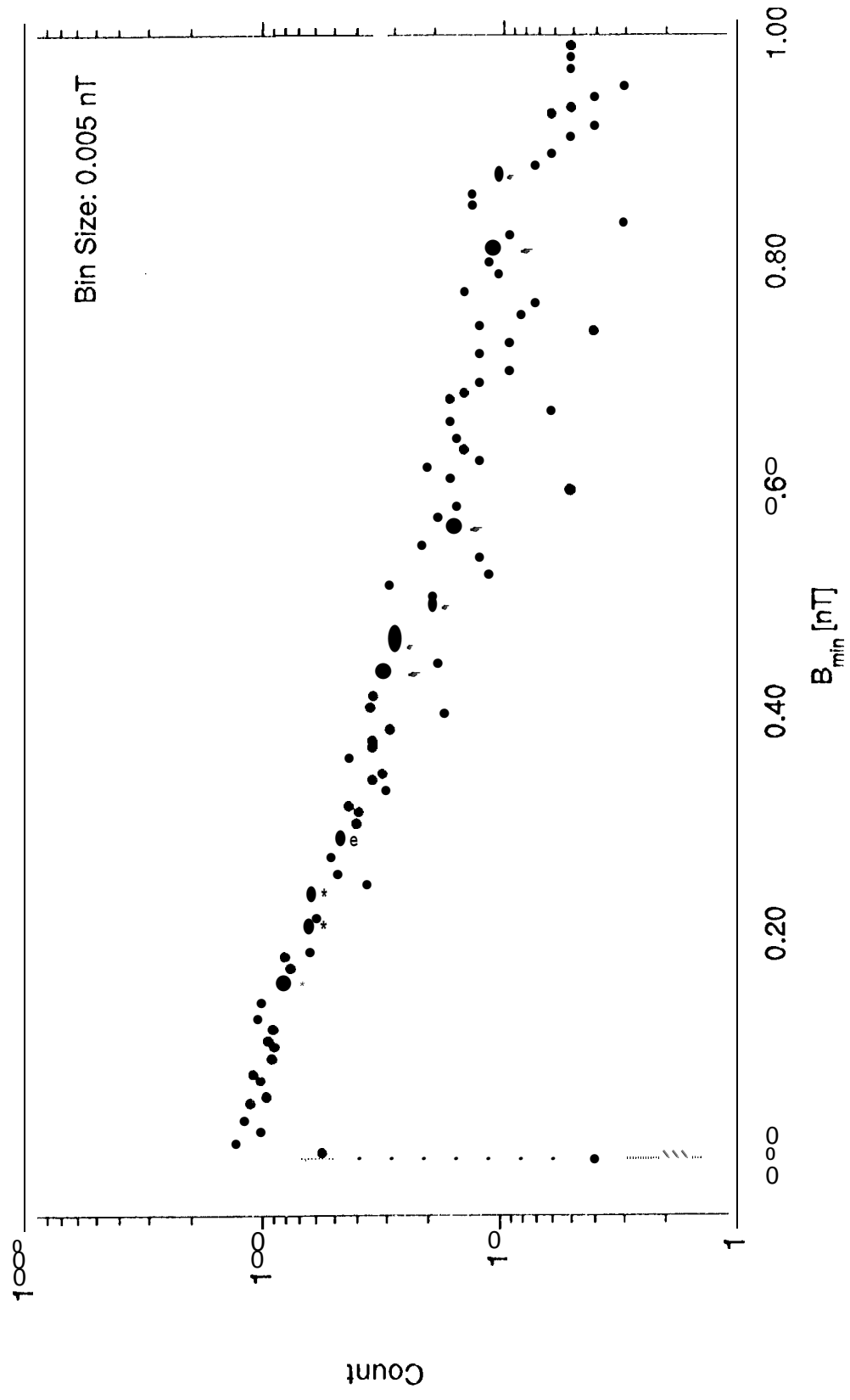


Figure 5

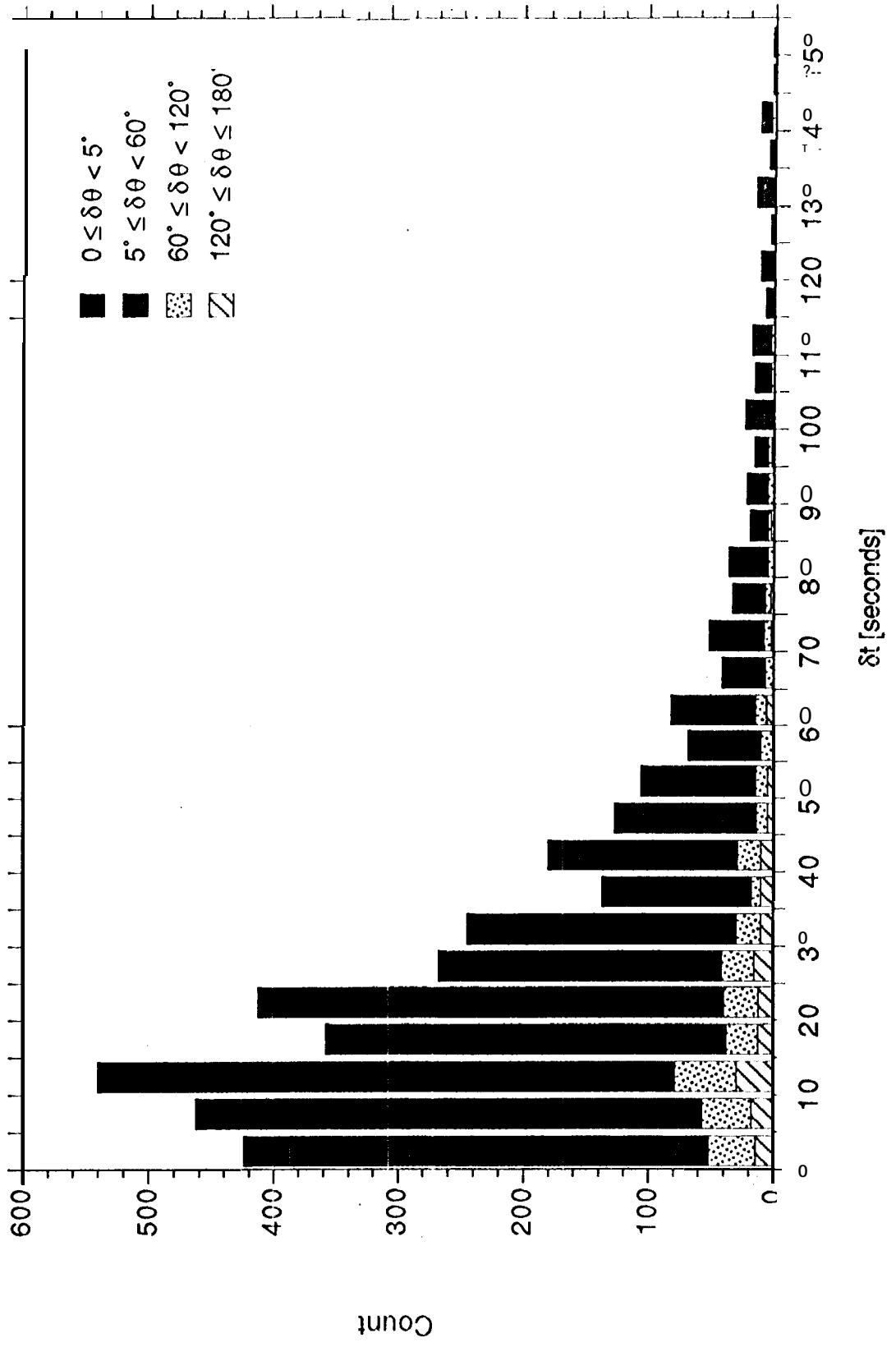
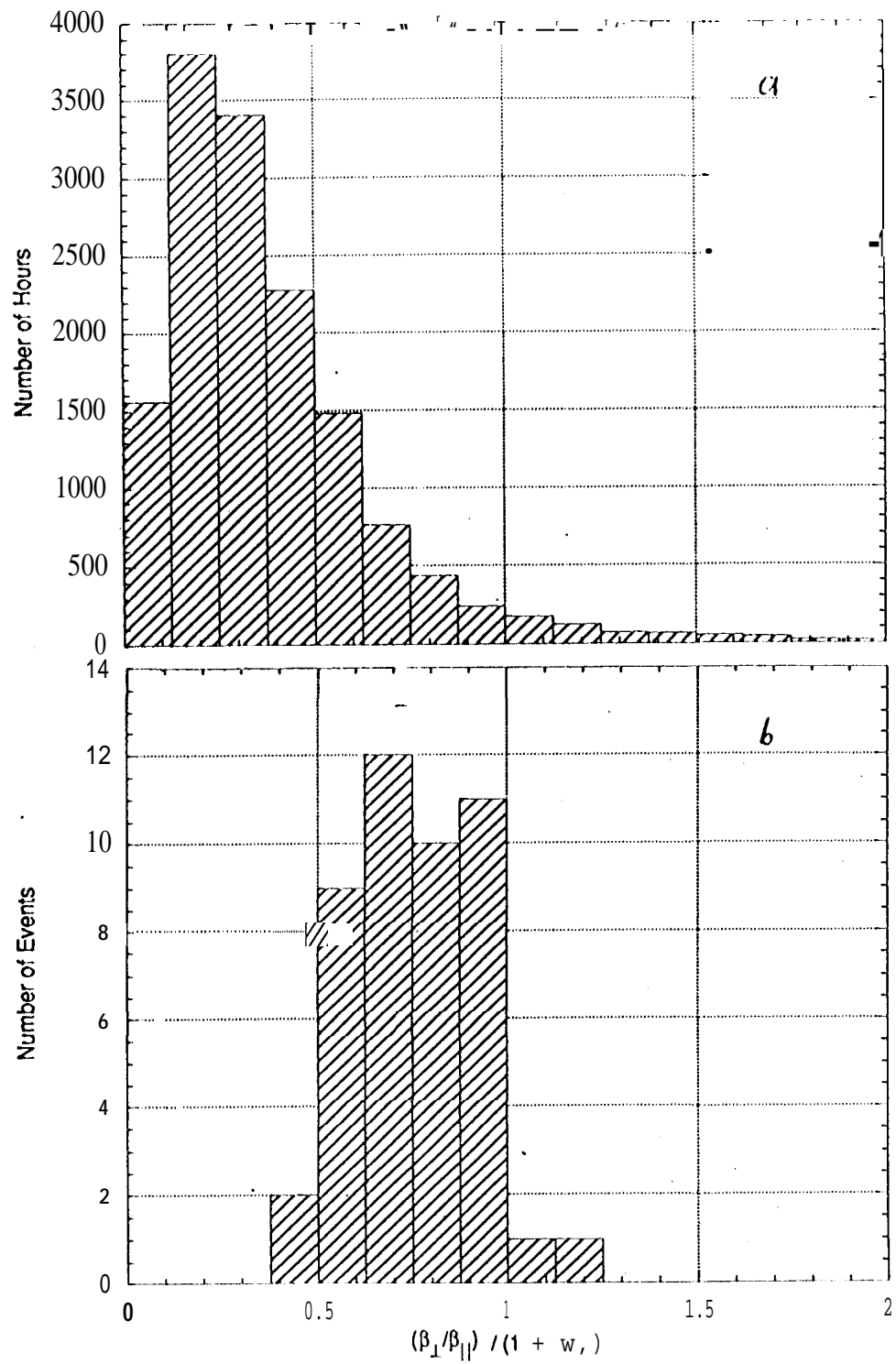
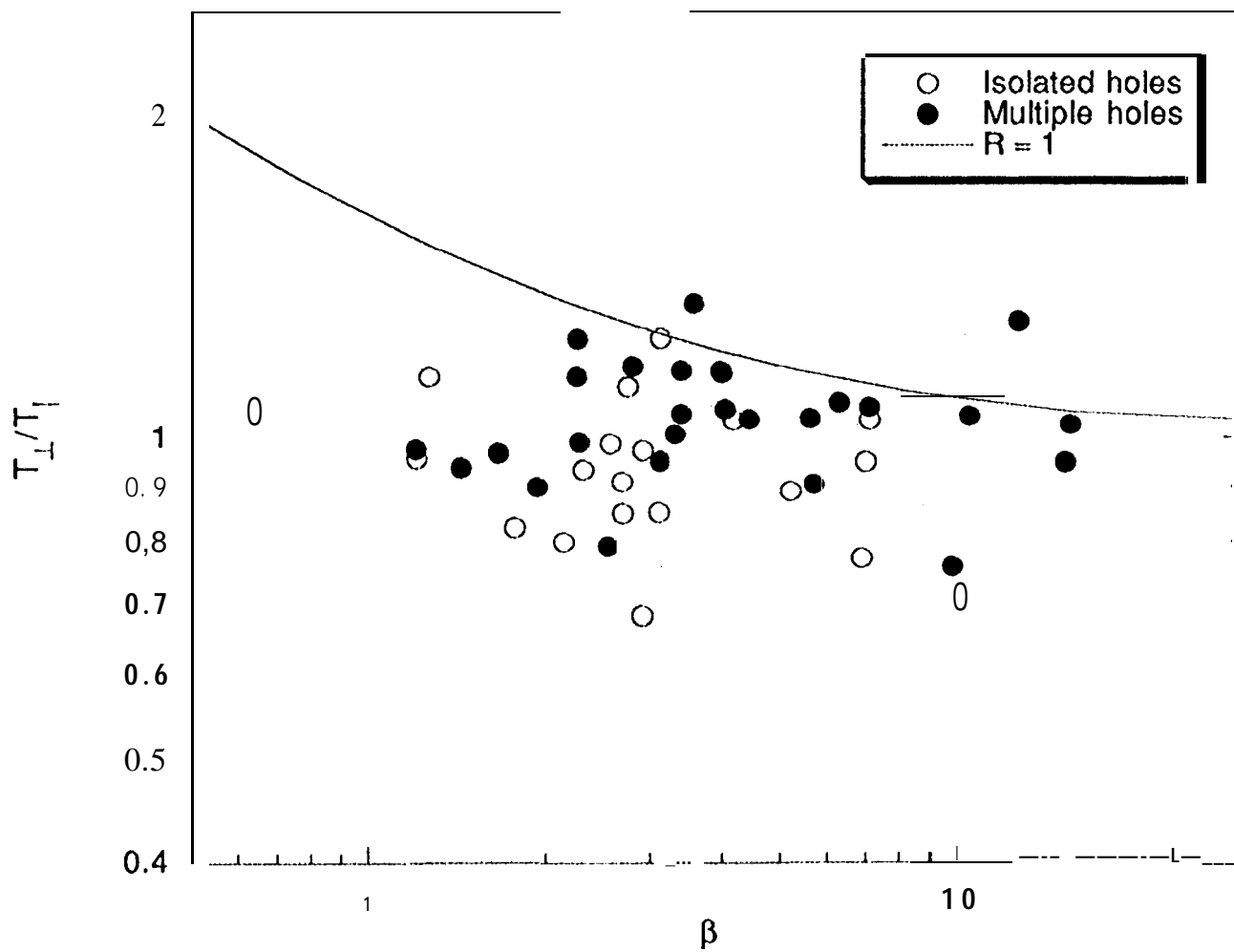
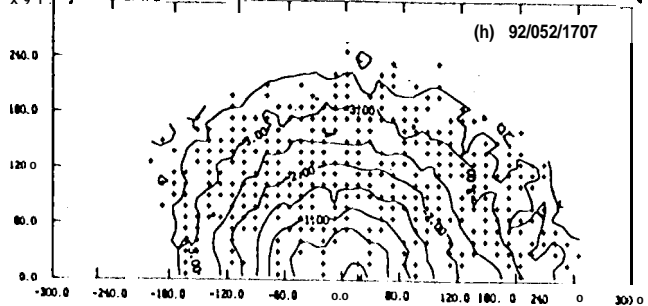
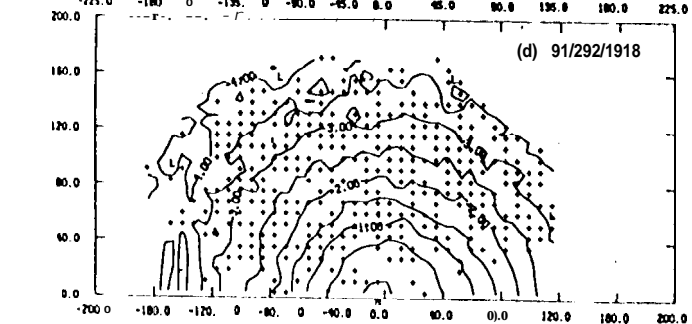
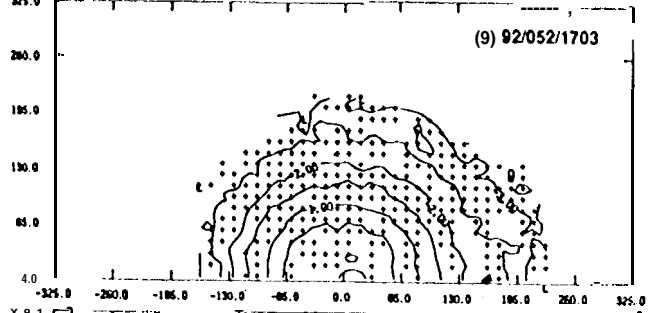
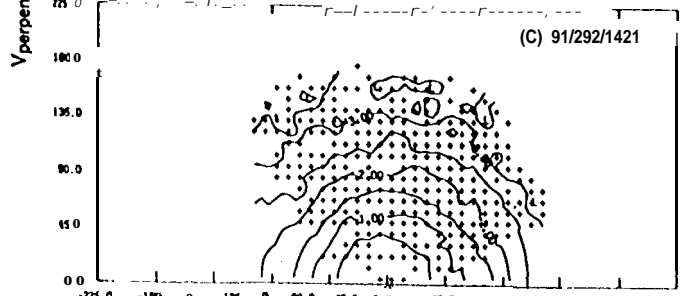
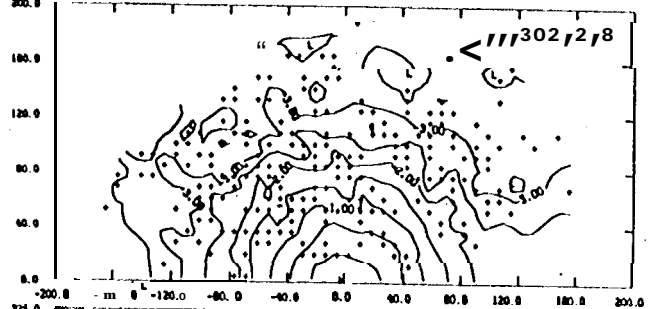
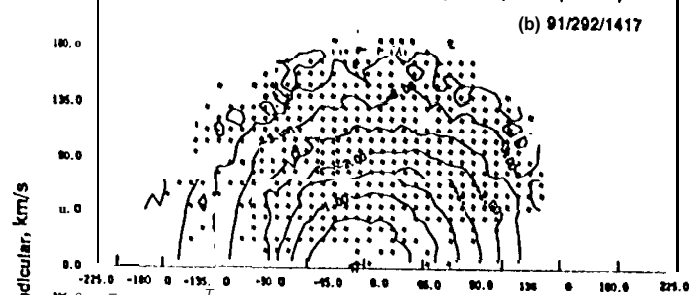
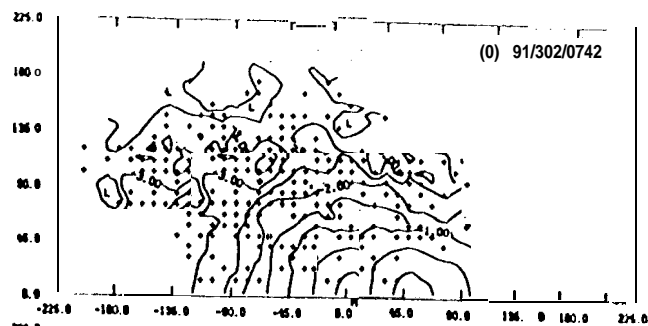
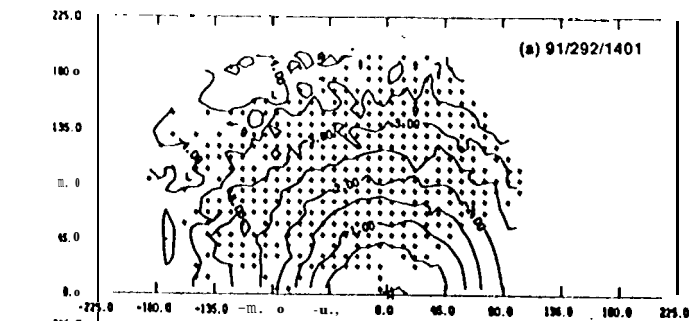


Figure 6







$V_{parallel}$, km/s

